HIGH ACCURACY METHODS FOR FOAM INJECTION-EXPANSION SIMULATION

G. François, Transvalor Company, Mougins, France
L. Ville, Transvalor Company, Mougins, France
N. Poulain, Transvalor Americas Company, Chicago
J. Claracq, DOW Company, Benelux

Abstract

In this paper, we propose a set of advanced numerical methods in order to simulate foam injection-expansion processes in a single step. Our approach is based on a set of stabilized solvers for each governing equation. These solvers are coupled with an advanced global stabilization algorithm and a multi-criteria adaptive meshing technology. These new technologies provide realistic results. We present several analytical and technical examples to demonstrate the overall robustness.

Introduction

Foam injection-expansion is nowadays a very widespread process, as it is used in a large variety of domains (automotive, everyday furniture …). In high precision domains such as automotive, it is necessary to better understand and control process. The use of an optimized numerical tool can help to find the best parameters to predict final foam distribution, and therefore optimize injected foam mass for example.

Foam injection-expansion is a complex process as several physical phenomena occur. Each phenomenon results of a complex equation and all together are highly coupled. Another difficulty appears in the fact that expansion occurs at the very beginning of the process, including filling step. Therefore every equation needs to be resolved with a high accuracy method, as a minor error could lead to poor final description.

In our work we use stable numerical method for each constitutive equation resolution. We propose as well a global stabilization parameter based on the overall mass conservation.

As foam injection-expansion processes are used for large and complex industrial parts, the use of advanced numerical methods is necessary to keep reasonable computations times. This is why we have also developed an anisotropic adaptive meshing technology. This technology enables us to improve results accuracy while decreasing computational time.

Finally we validate our methods through simple analytical cases as well as a more complex industrial part.

Constitutive Equations

Like any polymer, polyurethane foams are driven by Navier Stokes and heat equations:

$$\rho\left(\frac{\partial v}{\partial t} + v\nabla v\right) - \nabla\left(2\eta\varepsilon\left(v\right)\right) + \nabla p = f^{v} \tag{1}$$

$$\frac{d\rho}{dt} + \rho\nabla.v = 0 \tag{2}$$

where v is the velocity field (m/s), p is the pressure field (Pa), ρ is the polymer density (kg/m^3) and η is the polymer dynamic viscosity (Pa.s).

$$\frac{d(\rho c_P T)}{dt} = \nabla.\left(k\nabla T\right) + S \tag{3}$$

where T is the temperature (^{o}C), c_P is the calorific capacity (J/K/m^3), k is the heat conductivity coefficient (W/m²) and S is the source term (W/m^3) corresponding to viscous dissipation and polymerization reaction.

Gas rate produced by polymerization reaction is modeled by a ϕ parameter, as introduced in [1], it depends on temperature and pressure:

$$\frac{d\phi}{dt} = G\left(\phi, t, T\right) - \chi_P \frac{dP}{dt}\phi\left(1-\phi\right) \tag{4}$$
$$0 < \phi < 1$$

where $K(T)$ is a function depending on local temperature T, and χ_P is the foam compressibility.
Finally, foam expansion introduces a new term in conservation equation:

$$\frac{1}{\rho}\frac{d\rho}{dt} = \frac{1}{(1-phi)G\left(\phi, t, T\right)} - \chi_P \frac{dP}{dt} \tag{5}$$

Global Stabilization Method

In our work, Navier-Stokes equations are stabilized with a P1+/P1 method [2]. Heat equation and gas rate evolution equation are stabilized with a SUPG method[3].

Nevertheless, some inaccuracies may occur during computation. These inaccuracies can result from either non-convergence or poor discretization. Considering the fact that all equations are coupled together, this can lead to significant final discrepancies between computation and reality.

In order to ensure a good coherence between these equations, we define a global stabilization parameter f .This parameter is implemented in both conservation equation (1) and gas rate evolution equation (4):

$$\frac{1}{\rho}\frac{d\rho}{dt} = \frac{f}{(1-phi)\times G(\phi,t,T)} - \chi_p \frac{dp}{dt} \qquad (6)$$

$$\frac{d\phi}{dt} = G(\phi,t,T) - \chi_p f \frac{dp}{dt}(1-\phi) \qquad (7)$$

F is directly computed from discrepancy between overall computed mass and theoretically injected mass. For a optimum stability, we use a proportional et derivative scheme:

$$f(t) = \left(1 - \frac{1}{\alpha}\left(\frac{M_{th} - M(t)}{M(t)} + \tau \frac{1}{M}\frac{dM}{dt}\right)\right) \qquad (8)$$

Where α is the proportional parameter (we chose $\alpha = 0.1$), τ is the derivative parameter (we chose $\tau = 20\ \nabla t$) and M_{th} is the theoretical injected mass.

Anisotropic Adaptive Meshing

Our meshing technology is based on the so called "topological mesher" [4], that enables to generate highly anisotropic and heterogeneous meshes. Such meshes are very interesting for complex computations like industrial parts injection and expansion. Indeed, precision can be highly improved only in required directions (for example through thickness) and required zones.

The anisotropic mesher is coupled with the error estimator developed in [5]. The error estimator computes an optimized metric from one or several adaptation functions and a number of nodes. The obtained metric given to the mesher generates the computational mesh. Figure 1 gives an example of adaptation around the interface: this coupled with the level set function enables a very sharp interface description.

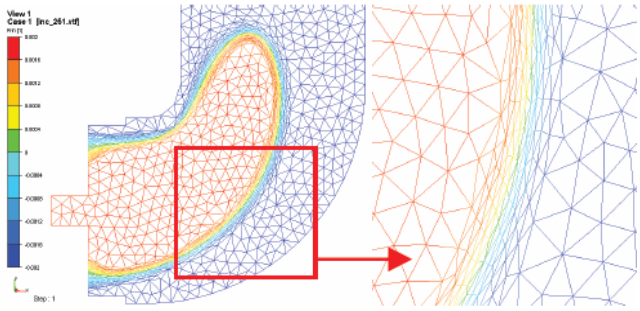

Figure 1. Anisotropic adaptive mesh with adaptation at the polymer/air interface.

Figure 2 shows that mesh can as well be refined following border conditions and velocity profile in order to improve heat transfers and flow/rheology coupling.

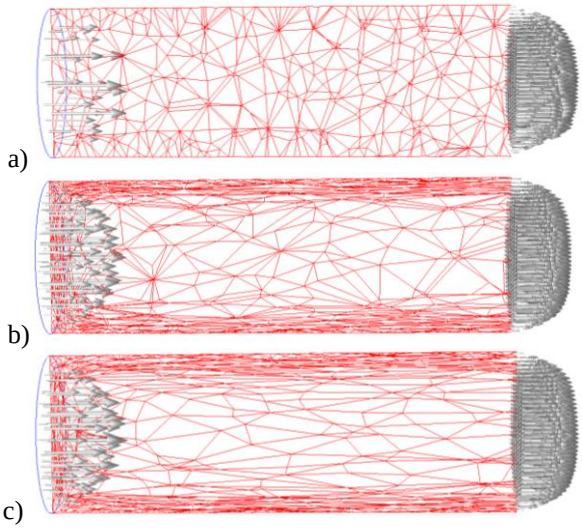

Figure 2. a) Isotropic homogeneous mesh; b) Refined on boundaries; c) Refined on boundaries and flow geometry.

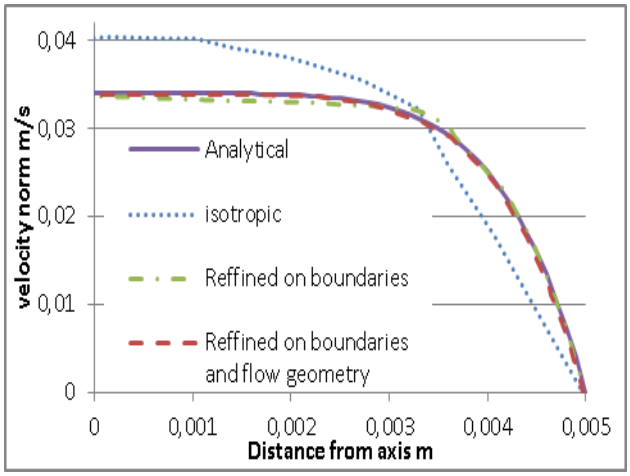

Graph 1. Pressure imposition in a tube: velocity profile with different mesh.

Graph 1 shows the results obtained for a pressure imposition on the left side. Adapting the mesh on boundaries and flow geometry greatly improves flow description.

Analytical Validation

The first case consists in a free air expansion in a cylindrical cavity (L=0.05m x R=0.005m). We are here interested in the evolution of the overall foam volume. Results shown on Graph 2 are compared to analytical data. In this case, we deliberately chose a coarse mesh to introduce numerical inaccuracies.

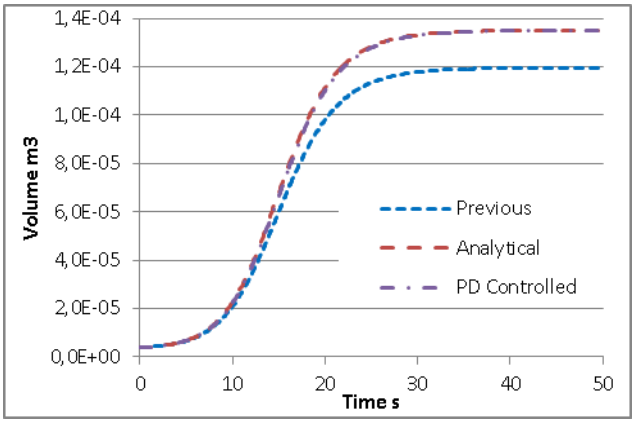

Graph 2. Evolution of overall foam volume with stabilized and non-stabilized resolution.

Here, the non-stabilized results show 15% discrepancy with the analytical results. Introducing global stabilization is enough to correct almost all the discrepancy.

The second test aims to validate the pressure dependency in the gas rate evolution function. We study here foam evolution in a fully confined cavity. As the polymerization occurs and foam is confined, only pressure should evolve and gas rate should remain steady.

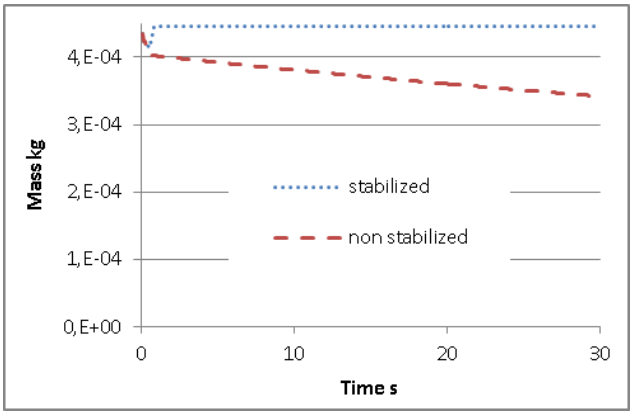

Graph 3. Evolution of overall foam mass in a fully confined cavity.

As the overall mass constantly decreases during the computation for non-stabilized case, the corrected case stabilizes quickly around its initial value.

Industrial Validation

In order to simulate complex industrial parts, we have introduced these methods in Rem3D® simulation tool [6]. For each simulation, injection and expansion are simultaneously resolved, as foam reacts from the very beginning of the process.

We validate our method on a large industrial part ($2x0.2x0.05m^3$) shown on Figure 3. During the two first seconds, a small amount (0.365kg) of non-expanded foam is injected into the cavity. The foam then expands and fills the whole cavity.

Figure 3. Industrial part geometry used for validation.

First, we decide to run computation with and without adaptive meshing in order to compare the interface aspect. Results are shown Figure 4. Both computation are launched with a 20,000 nodes mesh.

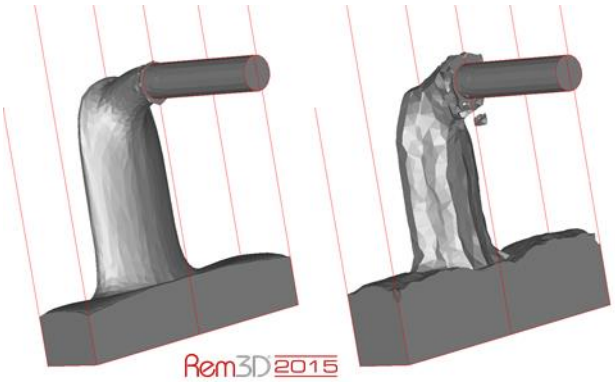

Figure 4. Interface description with adapted mesh (left side) and standard mesh (right side).

It appears that adaptive meshing greatly improves interface accuracy.

In a second step, we propose to compare mass evolution for these two cases without global stabilization.

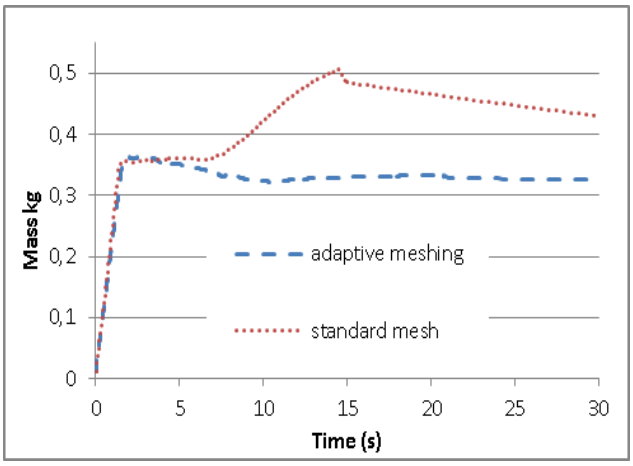

Graph 4. Influence of mesh adaptation on the overall foam mass evolution, without global stabilization.

It appears that both simulation show great discrepancy considering the injected mass. Despite of this, adaptive meshing shows better results than isotropic mesh.

We now add global stabilization to these two cases. Graph 5 shows the results for the four simulations.

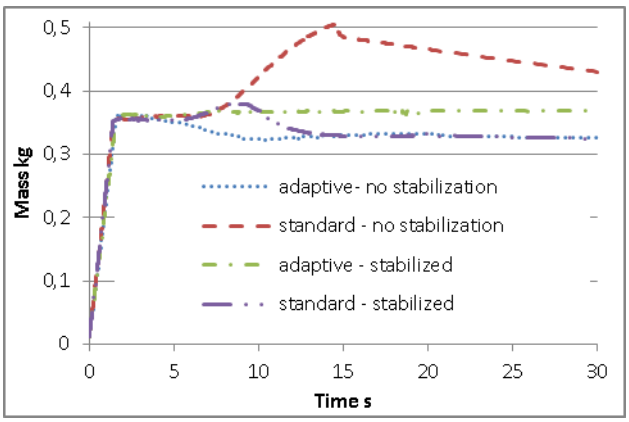

Graph 5. Influence of mesh adaptation and global stabilization on the overall foam mass evolution.

Finally, the stabilized adaptive meshing gives the most accurate description, as global stabilization is not sufficient to correct results obtained with the isotropic mesh.

Conclusions

In this paper, we have presented the different coupled equations driving foam injection-expansion. We have proposed a new global stabilization method in order to ensure a good coherence between all the phenomena.

In a second step, we presented our multi criteria adaptive meshing. This method enables us to improve accuracy while reducing computation time.

Finally, we used several analytical and industrial cases to demonstrate the overall code robustness and precision.

References

1. J. Bikard, J. Bruchon, T. Coupez and L. Silva, Numerical simulation of 3D polyurethane expansion during manufacturing process, *Colloids and Surfaces A : Physicochemical and Engineering Aspects*, **309**(1-3):49–63 (2007).
2. D.N. Arnold, F. Brezzi, and M. Fortin, A stable finite element for the stokes equations, *Calcolo*, **21** (1983).
3. R. Codina, Comparison of some finite element methods for solving the diffusion-convection-reaction equation, *Computer Methods in Applied Mechanics and Engineering*, **156**(1-4):185–210 (1998).
4. T. Coupez, H. Digonnet, R. Ducloux, Parallel meshing and remeshing, *Applied Mathematical Modelling*, **25**:153–175 (2000).
5. T. Coupez, Metric construction by length distribution tensor and edge based error for anisotropic adaptive meshing, *Journal of Computational Physics*, **230**:2391–2405 (2011).
6. G. François, Multi criteria adaptive meshing for polymers processing in Rem3D®, *30TH Polymer Processing Society* (2014).